Comparison of Pd and Pd_4S Based Catalysts for Partial Hydrogenation of External and Internal Butynes

Yanan Liu,[1,2] Yinwen Li,[1] James A. Anderson,[2] Junting Feng,[1] Antonio Guerrero-Ruiz,[3] Inmaculada Rodríguez-Ramos,[4] Alan J. McCue[5]* and Dianqing Li[1]*

[1] State Key Laboratory of Chemical Engineering, Beijing University of Chemical Technology, Beijing 100029, China.

[2] Surface Chemistry and Catalysis Group, Materials and Chemical Engineering, Department of Engineering, University of Aberdeen, Aberdeen, UK, AB24 3UE.

[3] Departamento de Química Inorgánica y Química Técnica, UNED, C/Senda del Rey 9, 28040, Madrid, Spain.

[4] Instituto de Catálisis y Petroleoquímica, CSIC, C/Marie Curie 2, 28049 Madrid, Spain

[5] Department of Chemistry, University of Aberdeen, Aberdeen, UK, AB24 3UE.

Tel: +44 1224 272838, Email: a.mccue@abdn.ac.uk, lidq@mail.buct.edu.cn

Abstract

The partial hydrogenation of but-1-yne and but-2-yne was studied with a view to probing the difference between external and internal alkynes. Catalysts with Pd and Pd_4S active phases were prepared on a carbon nanofiber support. Over the simple Pd catalyst over-hydrogenation was common which restricted alkene selectivity greatly – 25-35% depending on temperature. In contrast, the Pd_4S active phase offered exceptional alkene selectivity (maximum of 92-93% alkene selectivity for both the external and internal alkyne). DFT calculations were subsequently used to rationalise this difference in product selectivity – sulfur appears to change the geometry of the active site in Pd_4S and create a surface which favours alkene desorption relative to over-hydrogenation. This work further emphases the potential of palladium sulfide phases as an alternative to purely metallic palladium catalysts for partial alkyne hydrogenation.

Keywords

Partial hydrogenation, palladium sulfide, metal sulfide, but-1-yne, but-2-yne, butene

Introduction

Naphtha cracking remains one of the key methods for producing C1-4 alkene streams for use in polymer production. The process also yields small amounts of alkynes (*ca*. 5000-10000 ppm) which must be removed (typical requirements: < 10 ppm or > 99.9% conversion) otherwise they poison the downstream polymerisation catalysts [1,2,3]. Whilst this can in principle be achieved by sorption methods [4], the market size/value of the alkyne is relatively low. Therefore, the preferred method of removal is through selective hydrogenation to the corresponding alkene as this improves alkene yield and hence profitability. The challenge here lies in controlling selectivity since the alkene (either present in the feed stream or produced from the alkyne) is prone to over-hydrogenation to form the alkane. Industrially this is achieved using a bimetallic PdAg catalyst where Pd is the active phase and Ag acts as structural modifier [5,6]. A significant amount of research has focused on improving our fundamental understanding of how these catalysts function through both experimental and theoretical studies which point to the crucial role of Pd hydrides and/or carbides [7,8,9,10]. Numerous studies have also considered the development of alternative catalysts formulations with interesting options including alternative active metals [11,12], different bimetallics/intermetallics [13,14,15,16,17,18], surface or ligand modifications [19,20] and oxide catalysts [21]. In several cases, high selectivity is attributed to the geometry around the active site leading to the concept of ensemble design.

In terms of alkyne/alkene systems studied, the vast majority of works focus on the acetylene/ethylene system [1,22]. This may in part be related to historically high demands for polyethylene, although it should be acknowledged that the C2 system represents a simpler system to study conceptually and perhaps theoretically. In recent years, more literature has reported results from the propyne/propylene system which may, in part, be

related to increasing demand for polypropylene relative to polyethylene. In general, literatures show subtle differences in catalyst performance for these two streams with higher alkene selectivity more commonly reported for the C3 stream [21, 23 , 24]. Regardless, both acetylene and propyne represent terminal alkynes meaning that adsorption to a surface could occur end-on (i.e., vinyl, or vinylidene) or parallel to the surface (i.e., π-bonded or di-σ-bonded) [1]. Indeed, a number of difference surface species have been reported, although not all would be considered as the key reactive species [see reference 1 and therein].

Literature focusing on the C4 stream is much sparser with many studies looking at the hydrogenation of 1,3-butadiene or butenes. Remarkably little literature explores C4 alkynes which is perhaps surprising given that but-2-yne [25,26,27] and but-1-yne [28,29,30] represent a simple way to study the effect of triple bond position. Furthermore, different adsorption modes may be possible for but-1-yne (i.e., end-on or parallel) whereas but-2-yne is presumably restricted to something to akin to adsorption parallel to the surface. This in turn provides an interesting opportunity to probe the significance of active ensemble size/shape for alkyne hydrogenation catalysts. With butenes, both double bond shift and cis-trans isomerisation can also occur which can give further insight into catalytic properties [31,32].

One of the most promising alkyne hydrogenation catalyst formulations reported in recent years is based on palladium sulfide. In our group, we demonstrated that Pd_4S nanoparticles are exceptionally active and selective for gas phase alkyne hydrogenation, even under more challenging industrial conditions of moderate pressure [24,33,34]. It was postulated that performance was related to the nature of the active Pd sites created by neighbouring sulfur atoms. Albani *et al*. subsequently demonstrated that Pd_3S nanoparticles showed similar high performance for liquid phase alkyne hydrogenation and were able to relate performance to Pd ensembles using Density Functional Theory (DFT) calculations [35]. In this work, the performance of Pd_4S nanoparticles supported on carbon nanofibers (CNF) is reported for both but-1-yne and but-2-yne hydrogenation.

Results are compared with a more conventional Pd catalyst of similar particle size on the same carbon support. Catalytic tests indicate that the Pd_4S/CNF sample is highly effective at avoiding over-hydrogenation for both types of C4 alkyne. Furthermore, because lesser amounts of butane are formed over Pd_4S/CNF there is ample opportunity for butene isomerisation to occur. Results are rationalised based on DFT calculations.

Experimental

Catalyst samples

Pd and Pd_4S nanoparticles supported on carbon nanofibers (PR24-HHT, Applied Sciences Inc.) were prepared as described previously [24,34]. Briefly, Pd/CNF with a nominal loading of 1 wt% Pd was prepared by impregnation using a $PdCl_2$ precursor dissolved in concentrated HCl. Pd_4S/CNF with a nominal loading of 1 wt% Pd was prepared by impregnation using a $PdSO_4$ precursor dissolved in water. This sample was then subjected to reduction at 523 K in 10% H_2/N_2. This treatment has been previously shown to result in the formation of Pd_4S nanoparticles [24,33,34].

Characterisation

The catalysts studied in this work have been characterised in detail using Transmission electron microscopy (TEM), X-ray Photoelectron Spectroscopy (XPS), High Energy X-ray Diffraction (HEXRD), Temperature Programmed Desorption Mass Spectrometry (TPD-MS) and Temperature Programmed Reduction Mass Spectrometry (TPR-MS) with results reported elsewhere [24,33,34]. For the sake of brevity, only data which is pertinent to the results presented in this study are included.

TEM images of catalysts were collected using a JEOL JEM-2100 field-emission gun electron microscope operated at 200 kV. Samples were suspended on a carbon coated copper grid from an ethanol solution. The mean diameter (d) and the volume weighted average diameter (d_{VWA}) were calculated based on a minimum of 100 particles using the following equations where n_i is the number of particles with diameter d_i:

$$d\ (nm) = \frac{\sum_i n_i d_i}{\sum_i n_i} \qquad\qquad d_{VWA}\ (nm) = \frac{\sum n_i d_i^4}{\sum n_i d_i^3}$$

Catalyst Testing

Catalytic tests were conducted in a continuous flow, fixed-bed microreactor (9 mm diameter, Microactivity Reference, supplied by Micromeritics) at 1 bar using 50 mg catalyst diluted with silicon carbide (Aldrich, 200–450 mesh). Prior to the reaction, catalysts were reduced in 10% H_2/N_2 at 523 K for 1 h. The inlet gas stream was comprised of either 6000 ppm but-1-yne or but-2-yne diluted in nitrogen (pre-mixed cylinders supplied by BOC special gases). Hydrogen was then co-fed to give the desired H_2:reactant ratio with the total flow rate equating to a gas hourly space velocity (GHSV) of approximately 78000 h^{-1}. 5 h time on stream (TOS) was permitted for tests where temperature (323-473 K) or H_2/reactant ratio (1.7-13.3) was varied. For such experiments, conversion/selectivity is reported at the end of each 5 h period, although the corresponding time on stream plots can be found in the supporting information. Additional test data is presented over a 24 h period on stream to demonstrate longer term stability.

The products were analysed online using a gas chromatograph (Perkin-Elmer Clarus 580) equipped with an elite alumina capillary column and a Flame Ionisation Detector (FID). The conversion of the reactant was quantified as the amount reacted divided by the amount introduced. The selectivity to products (butenes and butane) was calculated as the amount produced divided by the amount of reactant consumed. Selectivity to oligomers (i.e., alkyne dimers or trimers) was calculated based on carbon balance, although some products (C8's) were detectable using the analytical methodology employed. In general, test data reported herein was at high or complete alkyne conversion meaning that evaluation of kinetic parameters is not appropriate. However, these conditions are well suited to assessing whether a catalyst is prone to over-hydrogenation and/or isomerisation of the resulting alkene. The conditions also tend to mirror industrial requirements where high alkyne conversion (> 99.9%) is a requirement for downstream processing.

DFT Calculations

The reaction process for the hydrogenation of but-1-yne or but-2-yne on Pd_4S surfaces was explored by DFT calculations with the Vienna Ab-initio Simulation Package (VASP) code [36]. The electrons and ions interaction were described using the projector augmented wave (PAW) method, including the spin polarization [37]. The generalized gradient approximation and the Perdew-Burke-Ernzerhof functional (GGA-PBE) describes the electron exchange and correlation energies for all systems [38]. Iterative solutions of the Kohn−Sham equations were expanded in a plane-wave basis set defined by a kinetic energy cutoff of 400 eV. The convergence criteria for the electronic self-consistent iteration and the maximum force on any ion were set as 10^{-4} eV and 0.03 eV/Å, respectively. The most stable configurations of the reactant and intermediates on Pd_4S were determined by the standard DFT minimization. The transition states for hydrogenation were computed by using the climbing image nudged elastic band (CINEB) method [39]. The vacuum layer was set to 15 Å to avoid interaction from adjacent cells. The Pd_4S (200) surfaces were modeled by *p* (2 × 2) supercells – the (200) surface was selected based on the surface planes identified from TEM measurements (see later). The slabs contain six atomic layers, where the three at the bottom were fixed and the three on the top were fully relaxed. For geometric optimization and the search for transition states, the Brillouin zone integration is performed with 3×3×1 k-point sampling. The optimized lattice constants for Pd_4S (5.195×5.195×5.669 Å) agree well with the experimental values (5.115×5.115×5.590 Å; ICSD 23865).

Results & Discussion

Catalyst samples

Catalytic data from Pd/CNF and Pd_4S/CNF samples are reported in this work. Whilst detailed characterisation of these samples has been reported elsewhere [24,33,34], some brief aspects are discussed here to help the reader place the subsequent results within a broader context. Both samples are supported on a commercially available carbon nanofiber (surface area = 32 m^2 g^{-1}) which possess a hollow core. Pd/CNF sample was

prepared by impregnation and representative TEM images are shown in Figure 1A-C. A broad range of particle sizes were observed for Pd/CNF (inset in Figure 1A). This gives a mean diameter of 6.7 nm (Table 1) and a volume weighted average diameter of *ca*. 18 nm. This later value correlates well with the crystallite size determined from High-Energy X-ray Diffraction (HEXRD) [34].

Pd_4S/CNF sample was prepared by impregnation with a $PdSO_4$ precursor. A subsequent reduction treatment at 523 K results in the loss of a portion of sulfur (as SO_2 or H_2S) to yield a Pd_4S phase. The loss of sulfur has been verified by TPR-MS studies whereas the formation of Pd_4S was followed by *in-situ* HEXRD [34]. An equivalent transformation has also been observed for an unsupported bulk phase palladium sulfide sample [40]. Typical TEM images of Pd_4S/CNF sample are shown in Figure 1D-F along with a narrower particle size distribution (Figure 1D – inset). The mean particle size for Pd_4S/CNF (4.4 nm) is slightly smaller than for Pd/CNF (Table 1), although this difference is not thought to be significant in terms of catalytic performance.

But-1-yne hydrogenation

Almost all catalytic data presented herein is reported at or close to 100% conversion and as such kinetic parameters are neither assessed nor discussed. These conditions are however beneficial for evaluating a catalysts tendency to over-hydrogenate butyne and/or isomerise a double bond. Figure 2 shows conversion and product distribution for both catalysts as a function of temperature using a 3-fold excess of hydrogen relative to but-1-yne. These plots are constructed from the final data point collected after 5 h TOS at each temperature. The equivalent TOS plots which show only minor changes in selectivity over that 5 h period can be found in the supplementary information as Figure S1.

Regardless of temperature, Pd/CNF is prone to over-hydrogenation (Figure 2A) with butane produced as the major product (75-95% depending on temperature). This is perhaps not surprising as this catalyst has been reported to show poor butene selectivity when 1,3-butadiene is used as reactant [34]. Two other aspects are worthy of comment.

Firstly, at 323 K the selectivity to trans-2-butene and cis-2-butene are 21 and 10%, respectively with only trace quantities of but-1-ene. In order for this selectivity pattern to be observed, but-1-yne must be hydrogenated to but-1-ene which either undergoes rapid hydrogenation to butane or isomerisation to but-2-enes (perhaps with subsequent hydrogenation). These results correlate with the expected thermodynamic stability (trans-2-butene > cis-2-butene > but-1-ene). For example, Bobylev *et al.* reported that at 333 K the equilibrium composition is *ca*. 65:31:4 trans-2-butene: cis-2-butene: but-1-ene [41]. Results reported here are also similar to those reported by Alves *et al*. for the liquid phase hydrogenation of but-1-yne over a commercial Pd/Al_2O_3 egg-shell catalyst [30]. The second point of note is how the product distribution changes with increasing temperature. As temperature increases, catalytic activity would be expected to increase leading to more alkane formation. However, beyond 423 K selectivity to alkenes actually increases. This is thought to be associated with the adsorption strength of the alkenes. In other words, as temperature increases, the alkene species have a shorter residence time meaning that secondary reactions are less likely to occur. Such an explanation seems plausible since the selectivity pattern at 473 K is the opposite of that expected based on equilibrium (i.e., but-1-ene > cis-2-butene > trans-2-butene).

Figure 2B displays the equivalent dataset for the Pd_4S/CNF catalyst. Again 100% conversion is observed across the entire temperature range, although conversion was seen to increase from approximately 60 to 100% over the first 4 h (Figure S1). In terms of product selectivity, Pd_4S/CNF is inherently more selective than Pd/CNF with a maximum butane selectivity of *ca*. 47% observed at 323 K. As temperature increases, butane selectivity decreases to < 5% at 423 K confirming that Pd_4S is a remarkably effective catalyst for avoiding over-hydrogenation. Improved butene selectivity at higher temperature (> 95% above 423 K) is again attributed to the alkenes adsorbing less strongly as temperature increases. Similar trends have been observed and reported for acetylene and propyne [24,33]. Across the entire temperature range, Pd_4S/CNF produces but-1-ene (35-46%) as the major product if cis and trans-2-butene are considered separately. This aspect is

particularly intriguing because in the absence of an alkyne or alkadiene, butenes would be expected to adsorb and isomerise to but-2-enes as seen for Pd/CNF (see Figure 2A). Therefore a catalyst which produces higher yields of but-1-ene may be of interest for processes which require a but-1-ene stream.

Based on the results described above, the sensitivity of both catalysts to hydrogen availability/excess were explored at 473 K since this was the temperature at which butane selectivity was lowest. Perhaps unexpectedly the butene selectivity over Pd/CNF (Figure 3A) is strongly related to hydrogen excess. With a 1.7-fold excess of hydrogen relative to but-1-yne alkene selectivity is *ca*. 67%, however this decreases stepwise as the hydrogen: but-1-yne ratio is increased until the cumulative butene selectivity is less < 5%. This trend is characteristic of a catalyst which is inherently unselective. In contrast, the data collected for Pd_4S/CNF (Figure 3B) remarkably shows that total alkene selectivity is almost unaffected by hydrogen excess. For example, butane selectivity with a 1.7-fold excess of hydrogen is approximately 1% and this only increases to 6% when the hydrogen excess is increased to 13.3-fold. Instead, hydrogen excess is seen to influence the distribution of the butenes more. In general, a higher hydrogen:but-1-yne ratio favours formation of the more thermodynamically stable trans-2-butene and cis-2-butene instead of 1-butene [41].

In order to assess the long-term stability of Pd_4S/CNF, a further test reaction was performed over a 24 h period at 473 K (data for Pd/CNF can be found as Figure S3). This dataset was collected using a 3-fold excess of hydrogen relative to but-1-yne and the data is presented in Figure 4. As a result of operating at 100% conversion it is not possible to comment on deactivation and instead only selectivity trends are discussed. Although in previous work it was demonstrated that Pd_4S/CNF only showed deactivation under extreme conditions (i.e., concentrated alkyne streams & abnormally high GHSV) [24]. Across the 24 h TOS period (Figure 4), product selectivity remains remarkably constant. One point of note is that under equivalent operating conditions of temperature and hydrogen excess the product distribution is subtly different in Figures 2 and 4. The data at 473 K in Figure 2 is collected after the catalyst has operated for 30 h total at 6 different temperatures. This difference

may be indicative of a 'memory effect' which may be associated with carbon retention on the catalyst surface. Indeed, it has been widely acknowledged that carbon deposition influences product selectivity in alkyne hydrogenation over Pd-based catalysts [1,22]. As such, this aspect requires further work and is the subject of on-going investigations.

DFT calculations for but-1-yne hydrogenation on Pd_4S

Why does the Pd_4S catalyst exhibit such high alkene selectivity for but-1-yne hydrogenation? In order to try and resolve this question, DFT calculations were performed using a model of the (200) surface plane of Pd_4S since lattice spacings consistent with this surface termination were observed by TEM (Figure 1). The full potential energy profile for the hydrogenation of but-1-yne on Pd_4S surface is presented in Figure 5. The corresponding computed energy barriers and the reaction energies are summarized in Table 2. The hydrogenation of but-1-yne follows Langmuir-Hinshelwood kinetics where C_4H_6 and H_2 molecules chemisorb on the active site and react via a series of hydrogen addition steps through a Horiuti-Polanyi like mechanism [42]. In detail, but-1-yne adsorbs from the gas phase onto two neighbouring Pd atoms with an adsorption energy of −1.59 eV (note: this type of site only exists because of the surface structure created by sulfur atoms). This therefore implies that the triple bond is adsorbed parallel to the surface. Adsorbed hydrogen atoms then add to the triple bond to generate but-1-ene *via* a butene-like C_4H_7Pd intermediate which is thermodynamically favoured. The kinetic barriers of the first two hydrogenation steps are calculated to be only 0.51 eV (TS1) and 0.47 eV (TS2), implying that Pd_4S/CNF is highly active. The C_4H_8 molecule is able to coordinate on the equivalent two Pd atom site via a di–σ bond with an adsorption energy of −1.02 eV. However, further hydrogenation of C_4H_8 to a C_4H_9 intermediate must pass through a large and presumably prohibitive barrier of 1.33 eV (TS3). Given that the desorption energy of C_4H_8 (1.02 eV) is lower than the energy of TS3 transition-state, desorption and/or isomerisation (not calculated) is preferred over further hydrogenation. These calculations therefore provide an explanation for the high alkene selectivity of Pd_4S/CNF in the partial hydrogenation of but-1-yne [43,44].

For comparison, we also make use of literature to consider reaction of acetylene (as the simplest external alkyne molecule) on a Pd (111) surface [45]. As presented in the full potential energy profile, acetylene molecules preferentially adsorb on the 3-fold coordinated hollow sites with adsorption energy of -2.02 eV, followed by hydrogenation of C_2H_2 to C_2H_4 via a C_2H_3* intermediate with an activation barrier of 0.72 eV (TS1) and 0.67 eV (TS2). The produced C_2H_4 molecule coordinates on Pd atoms via di-σ configuration with the desorption energy of 1.30 eV, much higher than its subsequent hydrogenation barrier (TS3, 0.52 eV), which generally agrees with the relatively low ethylene selectivity for a Pd (111) surface [45].

But-2-yne hydrogenation

An equivalent series of catalyst tests were also conducted using but-2-yne as a model internal alkyne. Figure 6A shows the effect of reaction temperature on product distribution for Pd/CNF. In terms of butane selectivity, the data looks very similar to that observed for but-1-yne with alkane selectivity decreasing at elevated temperature. What is perhaps surprising is that but-1-ene was the alkene produced with higher selectivity than either cis or trans-2-butene across the entire temperature range which seems counter-intuitive. In order for this to form, but-2-yne is first expected to form cis-2-butene which would need to undergo double bond shift. Whilst isomerisation is favoured by higher temperature, the but-2-enes are more thermodynamically stable than but-1-ene hence this is unexpected [41]. The product distributions over Pd_4S/CNF between 323 and 473 K are presented in Figure 6B. At 323 K, conversion was incomplete and limited to 69-74% (see Figure S2 for TOS plot). At this level of conversion, cis-2-butene was formed with highest selectivity which is consistent with it being the primary product of but-2-yne hydrogenation. At higher temperature (i.e., 373 K) complete but-2-yne conversion was observed and both cis-2-butene and trans-2-butene were formed in similar amounts. In keeping with data presented earlier, alkane selectivity was higher (*ca*. 30%) at low temperature and decreased notably at elevated temperature (3% at 473 K). Once again this highlights the exceptional ability of Pd_4S/CNF sample to avoid over-hydrogenation.

The influence of hydrogen:but-2-yne ratio on product distribution for Pd/CNF and Pd_4S/CNF is shown in Figure 7A and 7B, respectively. Again, 473 K was selected since the lowest butane selectivity was observed at this temperature. In keeping with expectation, Pd/CNF is very sensitive to the amount of hydrogen which is co-fed with more hydrogen favouring butane selectivity (< 2% butene selectivity at 473 K with a 13.3-fold excess of H_2). In stark contrast, hydrogen:but-2-yne ratio barely effects product selectivity over Pd_4S/CNF. For example, with a 13.3-fold excess of hydrogen relative to but-2-yne, the total butene selectivity amounts to 93% with only 6% butane and *ca.* 1% oligomer formation. The exceptional performance of Pd_4S/CNF is further exemplified by examining the TOS plot over a 24 h period (see Figure 8) where the product distribution essentially appears constant (the equivalent plot for Pd/CNF can be seen in Figure S3B).

DFT calculations for but-2-yne hydrogenation on Pd_4S

As before, DFT calculations were used to reveal the process of but-2-yne hydrogenation on the Pd_4S (200) surface. Figure 9 shows the calculated energy profile and the corresponding geometric structures for but-2-yne hydrogenation (energy barriers and reaction energies are tabulated in Table 2). On the Pd_4S (200) surface, the most favourable adsorption site for but-2-yne is again two neighbouring Pd atoms which protrude from the surface plane. As expected, but-2-yne adsorbs with the C-C axis parallel to the surface, although the calculated geometry suggests an element of strain meaning that the molecule adopts a cis-type configuration once adsorbed. This step occurs with an adsorption energy of -1.74 eV. The hydrogenation of but-2-yne can then proceed via the addition of hydrogen to the C≡C bond in the two centre transition state as depicted (Figure 9). The C-C bond length linked to the surface increases from 1.21 Å in but-2-yne to 1.39 Å in the transition state as C_4H_7* begins to form. The activation barrier for this step (TS1) is calculated to be 0.15 eV. The subsequent hydrogenation of C_4H_7* intermediate to form cis-2-butene exhibits a barrier of 0.32 eV (TS2), which agrees with the data at 323 K presented in Figure 6B (i.e., cis-2-butene is the primary product). The desorption energy of C_4H_8 product is 1.19 eV, which is lower than the further hydrogenation barrier of 1.35 eV (TS3) which means

desorption is favoured instead of further hydrogenation which accounts for the excellent selectivity. Whilst further hydrogenation is not favoured, cis-2-butene isomerisation is known to occur (note: this aspect was not calculated by DFT).

Linking catalyst structure, testing and DFT calculations

A clear difference between the performance of Pd/CNF and Pd_4S/CNF catalysts was observed in this work. A simple Pd catalyst is inherently unselective and prone to over-hydrogenation regardless of whether the initial reactant was an internal or external alkyne. In contrast supported Pd_4S nanoparticles were shown to be selective for both types of alkyne. These results are in agreement with our own [24,33,40] and those of Albani *et al*. [35] which show that palladium sulfide based materials offer exceptional selectivity for alkyne hydrogenation for both simple and functionalised alkynes. Through the use of DFT calculations Albani et al. were able to relate selectivity to the size and geometry of the active sites created in sulfide materials – in that work Pd trimers were assigned as the key site [35]. DFT calculations in this work also suggest the geometry of the active site is important, although both alkynes initially adsorb via two adjacent Pd atoms protruding from the surface. Therefore, whilst a trimer of Pd atoms may exist on the surface layer, the uneven nature of the surface layer favours a dimer as the active site. It is therefore interesting to note that this type of ensemble design is spacious enough to bind both but-1-yne and the inherently bulkier but-2-yne. This contrasts the simple Pd catalyst which appears to offer up larger and more accessible adsorption sites which can be tuned in industrial catalysts by alloying with a second metal, where the second metal acts as a structural modifier [1,2,5,6]. Product selectivity, or specifically the limited ability of Pd_4S to over-hydrogenate can be rationalised by the relative energy barriers for desorption of the alkene and further hydrogenation. For both but-1-yne and but-2-yne, desorption is energetically favoured over further hydrogen addition which explains the exceptional alkene selectivity.

Conclusions

The performance of Pd/CNF and Pd_4S/CNF catalysts have been evaluated for the partial hydrogenation of butynes. Regardless of whether the substrate was an internal or external alkyne, Pd/CNF catalyst favoured over-hydrogenation to form butane. In contrast, Pd_4S/CNF offered exceptional performance with > 90% butene selectivity observed at 473 K for both but-1-yne and but-2-yne. In order to rationalise the exceptional performance of the Pd_4S/CNF catalyst, DFT calculations were performed. Through computational results it was possible to show that the energy barrier for desorption is lower than that for hydrogen addition to an alkane over a Pd_4S surface. Calculated adsorption geometries also hint that the active ensemble size and shape plays a role in controlling selectivity.

Acknowledgements

This work was supported by the National Natural Science Foundation of China and the Fundamental Research Funds for the Central Universities (buctrc201921).

Tables

Table 1 - Mean particle size (d) and volume–surface mean particle size (d_{VWA}) estimated from TEM measurements.

Materials	**Nominal metal loading (wt. %)**	**TEM**	
		$\Sigma n_i d_i / \Sigma n_i$ (nm)	**$\Sigma n_i d_i^4 / \Sigma n_i d_i^3$ (nm)***
Pd/CNF	1.0	6.7	18.3
Pd_4S/CNF	1.0	4.4	17.1

*Data from reference 34

Table 2 - Table of calculated energy barriers in eV on Pd_4S (200) surfaces. Equivalent values for the Pd (111) surface are from existing literature.

Process of hydrogenation	**But-1-yne**	**Aceylene**	**But-2-yne**
	Pd_4S	Pd[a] [45]	Pd_4S
C_4H_6 (g) + * ↔C_4H_6*	-1.59	-2.02	-1.74
C_4H_6* + H* ↔C_4H_7* + *	0.51	0.72	0.15
C_4H_7* + H*↔ C_4H_8* + *	0.47	0.67	0.32
C_4H_8* ↔C_4H_8 (g) + *	1.02	1.30	1.19
C_4H_8* + H* ↔C_4H_9* + *	1.33	0.52	1.35
C_4H_9* + H* ↔C_4H_{10}* + *	0.92	0.50	0.40

[a] Hydrogenation of external alkyne (acetylene) on Pd (111) surface

Figures

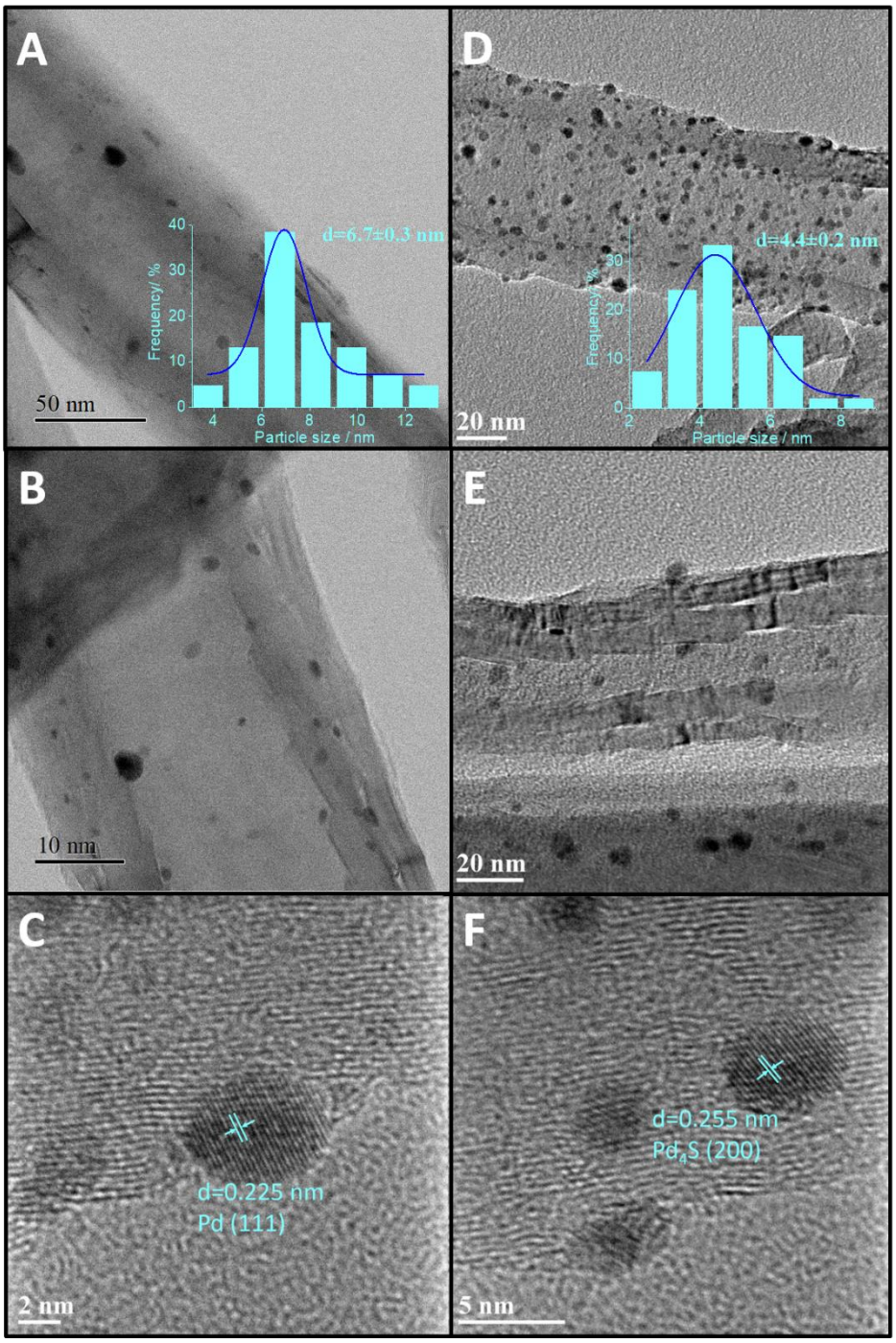

Figure 1 - HRTEM micrographs and associated particle size distributions histograms inset for Pd/CNF (A, B & C) and Pd_4S/CNF (D, E & F). Samples were pre-reduced *ex-situ* at 523 K prior to image collection.

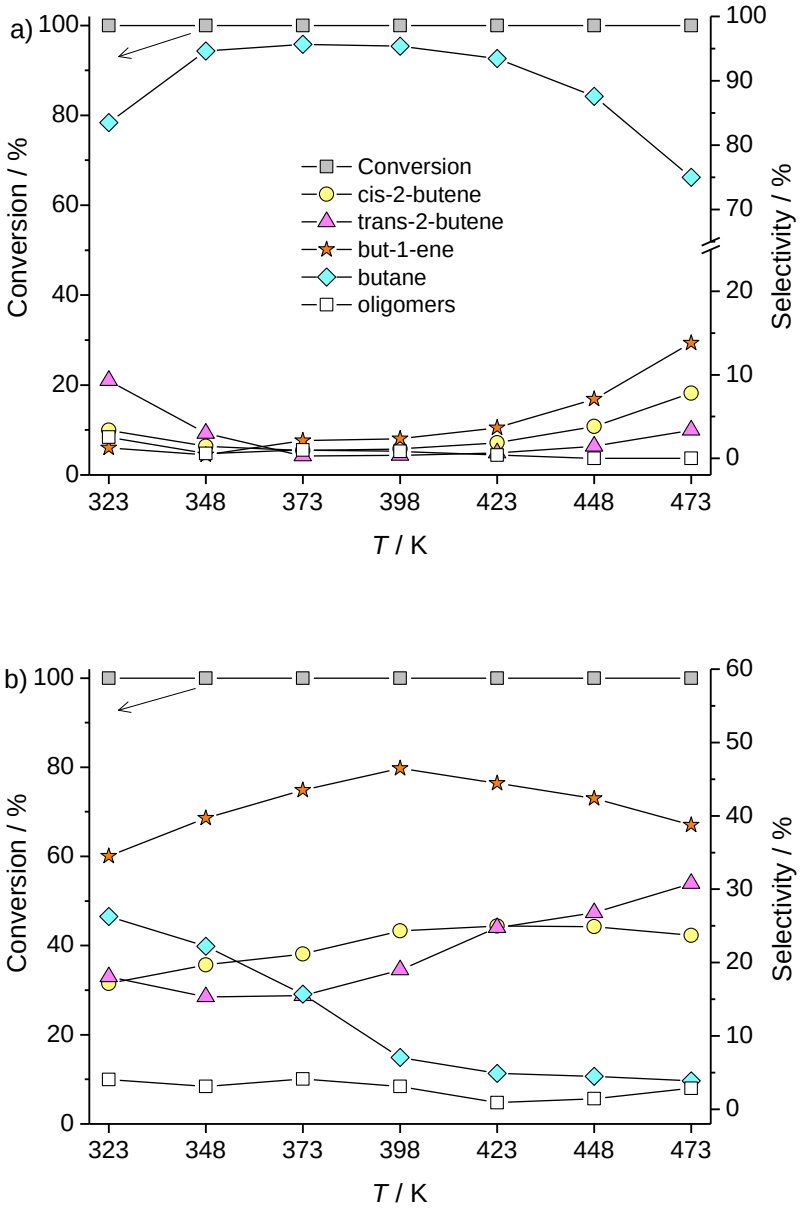

Figure 2 – But-1-yne conversion (grey squares) and product selectivity (see legend inset in figure) as a function of temperature over a) Pd/CNF and b) Pd_4S/CNF. Reaction conditions: 1 bar, H_2:but-1-yne ratio = 3:1, GHSV = 78000 h^{-1}, data shown after 5 h TOS.

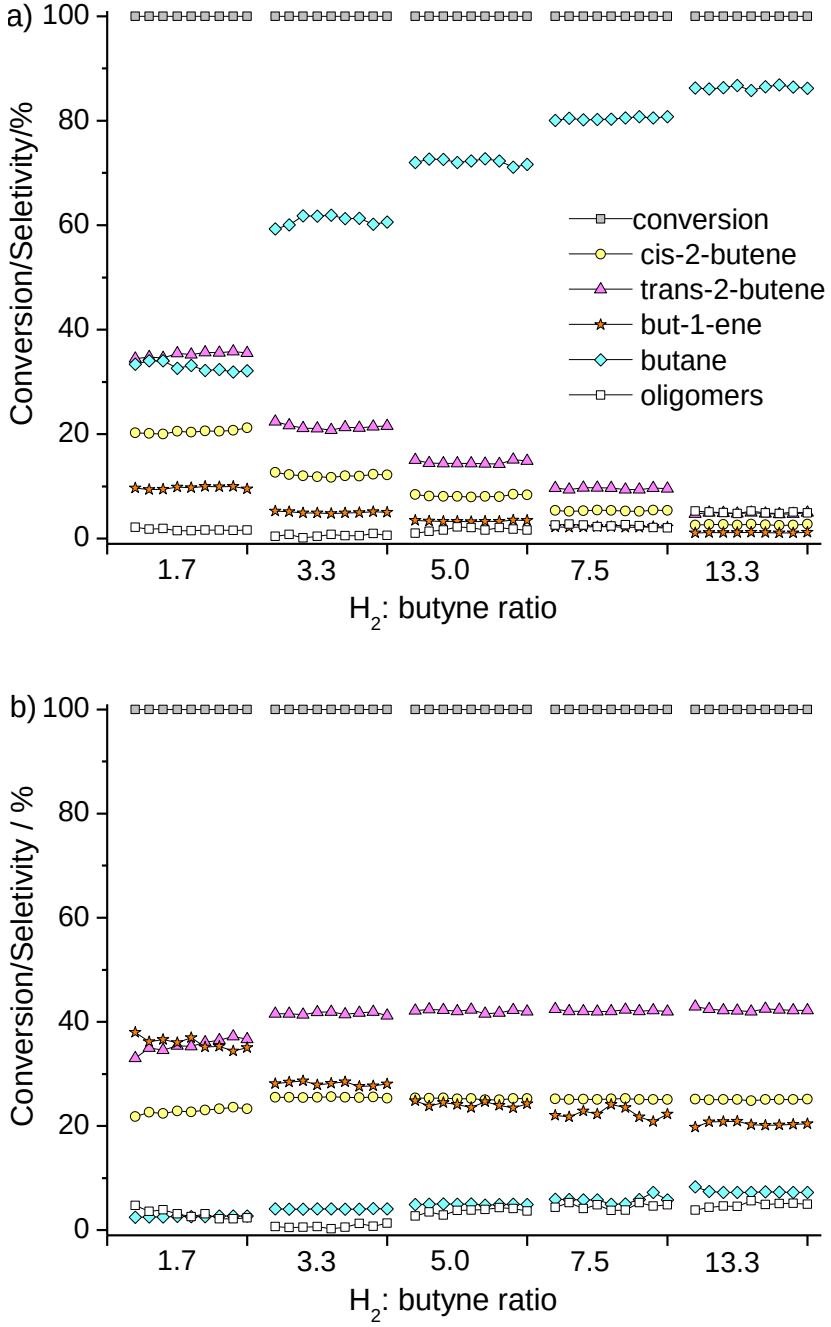

Figure 3 – But-1-yne conversion (grey squares) and product selectivity (see legend inset in figure) as a function of H_2:but-1-yne ratio over a) Pd/CNF and b) Pd_4S/CNF at 473 K. Reaction conditions: 1 bar, GHSV = 78000 h^{-1}, data shows 5 h TOS.

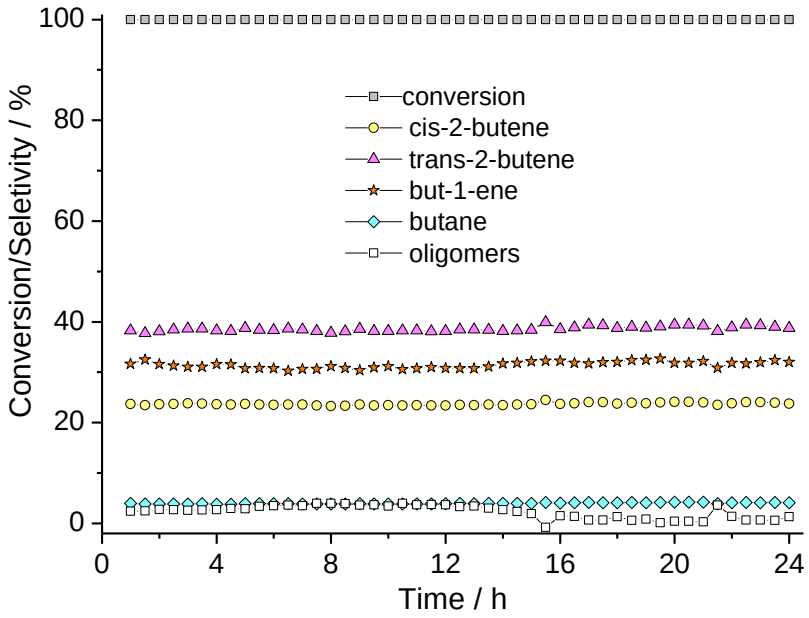

Figure 4 – But-1-yne conversion (grey squares) and product selectivity (see legend inset in figure) over Pd_4S/CNF at 473 K. Reaction conditions: 1 bar, H_2: but-1-yne ratio = 3:1, GHSV = 78000 h^{-1}, data shows 24 h TOS.

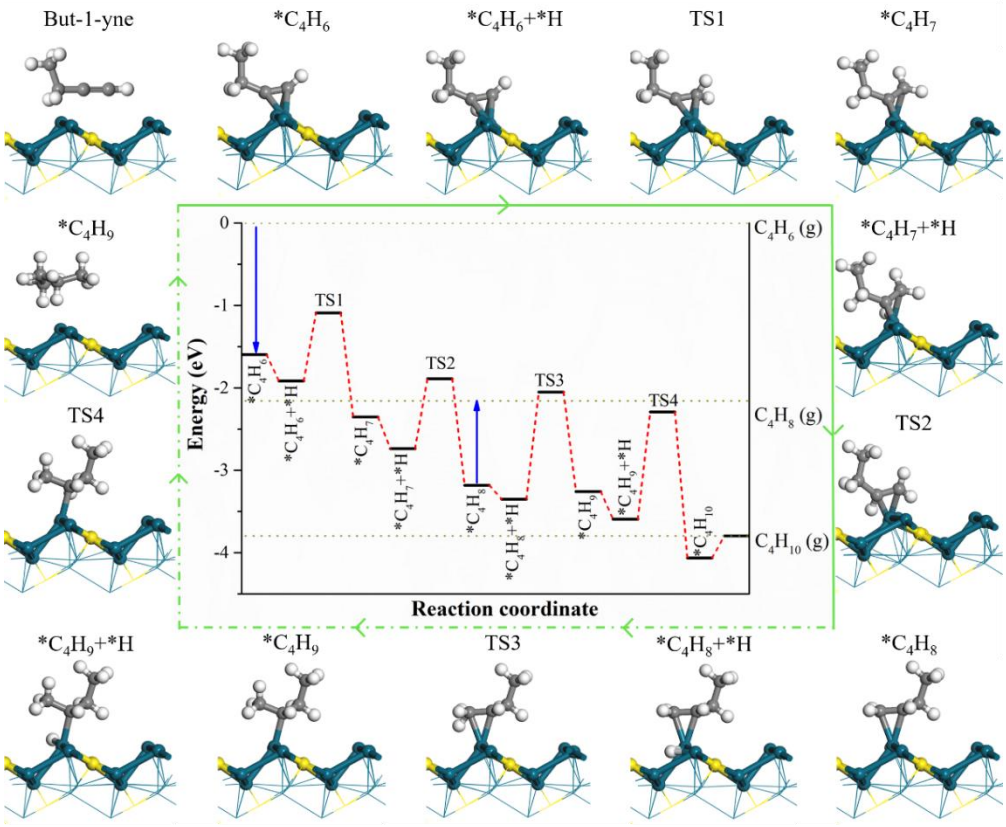

Figure 5 – Step-by-step hydrogenation mechanism of but-1-yne to butane on the Pd_4S (200) surface.

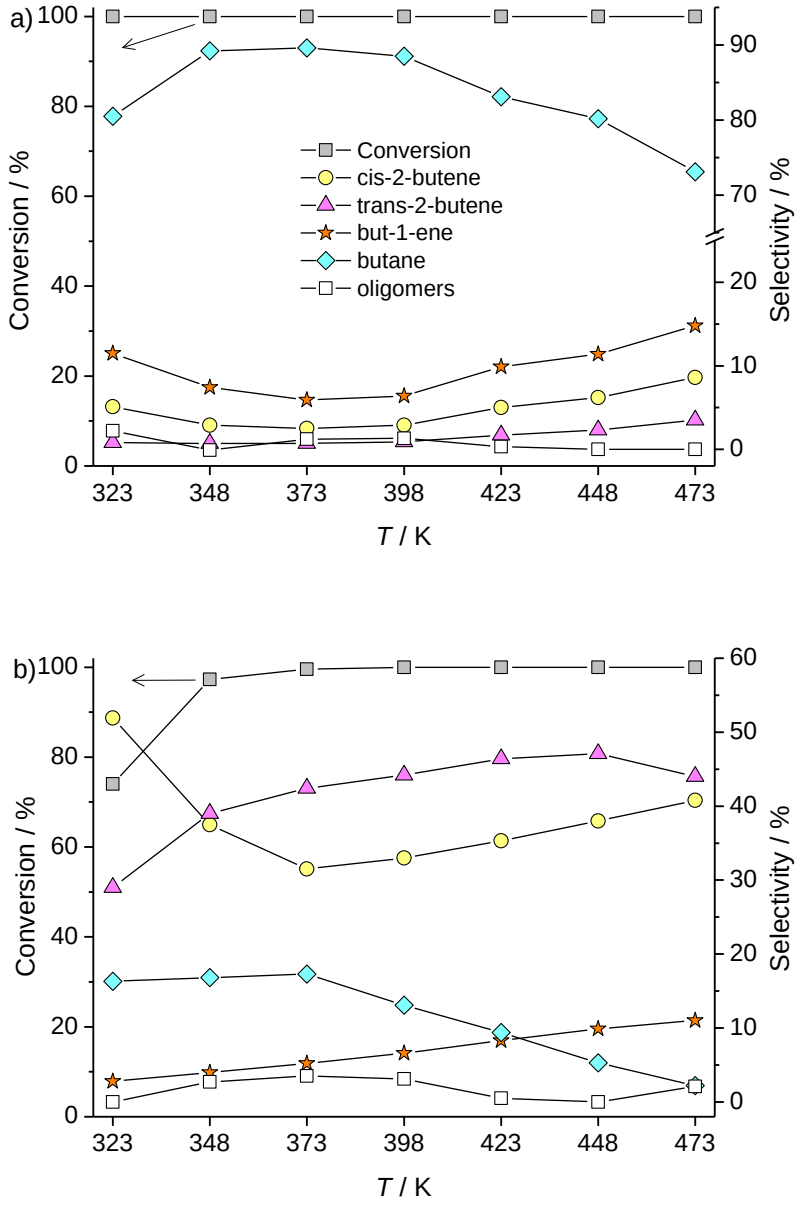

Figure 6 – But-2-yne conversion (grey squares) and product selectivity (see legend inset in figure) as a function of temperature over a) Pd/CNF and b) Pd_4S/CNF. Reaction conditions: 1 bar, H_2: but-2-yne ratio = 3:1, GHSV = 78000 h^{-1}, data shown after 5 h TOS.

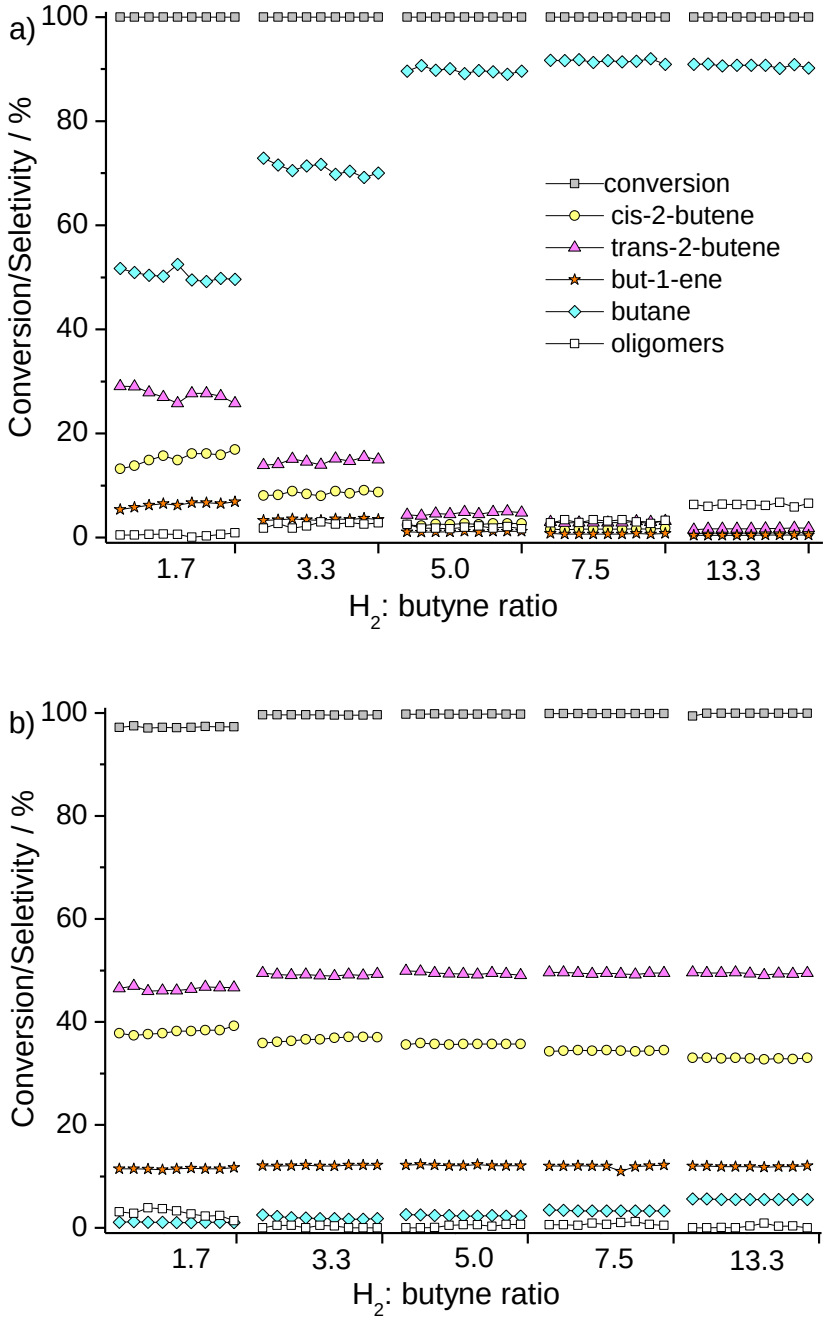

Figure 7 – But-2-yne conversion (grey squares) and product selectivity (see legend inset in figure) as a function of H_2:but-2-yne ratio over a) Pd/CNF and b) Pd_4S/CNF at 473 K. Reaction conditions: 1 bar, GHSV = 78000 h^{-1}, data shows 5 h TOS.

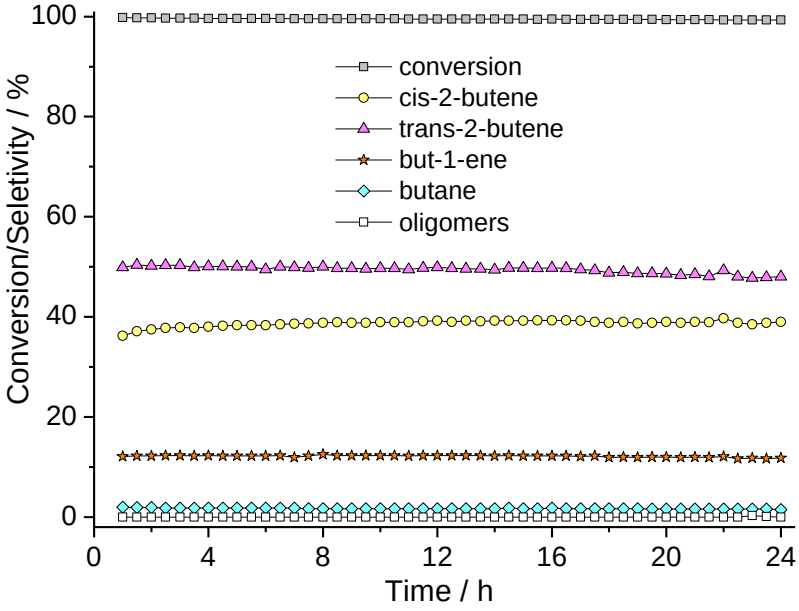

Figure 8 – But-2-yne conversion (grey squares) and product selectivity (see legend inset in figure) over Pd_4S/CNF at 473 K. Reaction conditions: 1 bar, H_2:but-2-yne ratio=3:1, GHSV = 78000 h^{-1}, data shows 24 h TOS.

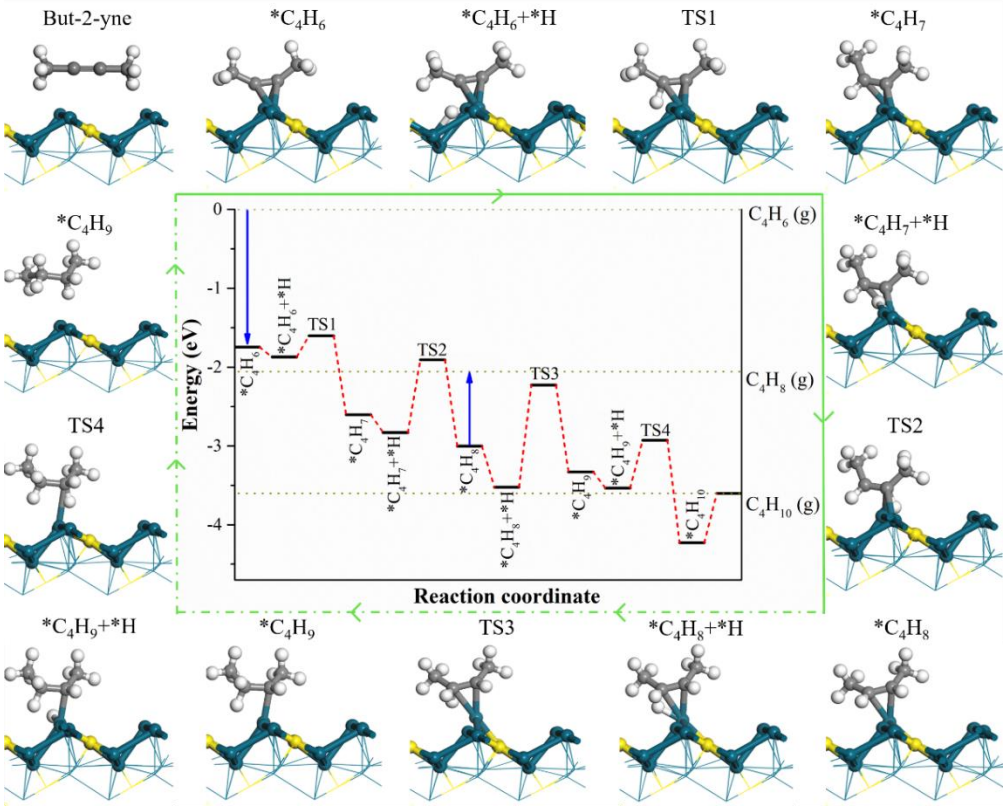

Figure 9 – Step-by-step hydrogenation mechanism of but-2-yne to butane on the Pd_4S (200) surface.

References

[1] A. Borodziński, G.C. Bond, Catal. Rev. 48 (2006) 91–144.

[2] S.A. Nikolaev, I.L.N. Zanaveskin, V.V Smirnov, V.A. Averyanov, K.I. Zanaveskin, Russ. Chem. Rev. 78 (2009) 231–247.

[3] A.J. McCue, J.A. Anderson, Front. Chem. Sci. Eng. 9 (2015) 142–153.

[4] L. Li, R-B. Lin, R. Krishna, X. Wang, B. Li, H. Wu, J. Li, W. Zhou, B. Chen, J. Am. Chem. Soc. 139 (2017) 7733-7736.

[5] A. Pachulski, R. Schödel, P. Claus, Appl. Catal. A Gen. 400 (2011) 14–24.

[6] M. Kuhn, M. Lucas, P. Claus, Ind. Eng. Chem. Res. 54 (2015) 6683–6691.

[7] N.A. Khan, S. Shaikhutdinov, H.J. Freund, Catal. Letters. 108 (2006) 159–164.

[8] W. Ludwig, A. Savara, K.H. Dostert, S. Schauermann, J. Catal. 284 (2011) 148–156.

[9] M. García-Mota, B. Bridier, J. Pérez-Ramírez, N. López, J. Catal. 273 (2010) 92–102.

[10] M. Armbrűster, M. Behrens, F. Cinquini, K. Föttinger, Y. Grin, A. Haghofer, B. Klötzer, A. Knop-Gericke, H. Lorenz, A. Ota, S. Penner, J. Prinz, C. Rameshan, Z. Révay, D. Rosenthal, G. Rupprechter, D. Teschner, D. Torres, R. Wagner, R. Widmer, G. Wowsnick, ChemCatChem 4 (2012) 1048-1063.

[11] S.A. Nikolaev, V.V. Smirnov, Catal. Today 147S (2009) S336-S341.

[12] B. Bridier, N. López, J. Pérez-Ramírez, J. Catal 269 (2010) 80-92.

[13] G. Kyriakou, M. B. Boucher, A. D. Jewell, E. A. Lewis, T. J. Lawton, A. E. Baber, H. E. Tierney, M. Flytzani-Stephanopoulos, E. C. H. Sykes, Science 335 (2012) 1209-1212.

[14] A. J. McCue, A. Gibson, J. A. Anderson, Chem. Eng. J. 285 (2016) 384–391.

[15] A .J. McCue, A. M. Shepherd, J. A. Anderson, Catal. Sci. Technol. 5 (2015) 2880–2890.

[16] A. J. McCue, J. A. Anderson, J. Catal. 329 (2015) 538–546.

[17] Osswald J, Giedigkeit R, Jentoft R E, Armbrüster M, Girgsdies F, Kovnir K, Ressler T, Grin Y, Schlögl R, J. Catal. 258 (2008) 210–218.

[18] Osswald J, Kovnir K, Armbrüster M, Giedigkeit R, Jentoft R E, Wild U, Grin Y, Schlögl R, J. Catal. 258 (2008) 219–227.

[19] F.M. McKenna, J.A. Anderson, J. Catal. 281 (2011) 231-240.

[20] A.J. McCue, F.M. McKenna, J. Anderson, Catal. Sci. Technol. 5 (2015) 2449-2459.

[21] G. Vilé, B. Bridier, J. Wichert, J. Pérez-Ramírez, Angew. Chem. Int. Ed. 51 (2012) 8620–8623.

[22] A. Borodziński, G.C. Bond, Catal. Rev. 50 (2008) 379-469.

[23] B. Bridier, J. Pérez-Ramírez, J. Am. Chem. Soc. 132 (2010) 4321-4327.

[24] A. McCue, A. Guerrero-Ruiz, I. Rodríguez-Ramos, J. A. Anderson, J. Catal. 340 (2016) 10-16.

[25] G. Webb, P.B. Wells, Trans. Faraday Soc. 61 (1965) 1232-1245.

[26] H.G. Rushford, D.A. Whan, Trans. Faraday Soc. 67 (1971) 3577-3584.

[27] S.D. Jackson, G.D. McLellan, G. Webb, L. Conyers, M.B.T. Keegan, S. Mather, S. Simpson, P.B. Wells, D.A. Whan, R. Whyman, J. Catal. 162 (1996) 10-19).

[28] J.P. Boitiaux, J. Cosyns, E. Robert, Appl. Catal. 32 (1987) 145-168.

[29] J.A. Alves, S.P. Bressa, O.M. Martinez, G.F. Barreto, Chem. Eng. Res. Des. 89 (2011) 384-397.

[30] J.A. Alves, S.P. Bressa, O.M. Martinez, G.F. Barreto Ind. Eng. Chem. Res. 52 (2013) 5849-5861.

[31] B. Brandt, J-H. Fischer, W. Ludwig, J. Libuda, F. Zaera, S. Schauermann, H.J. Freund, J. Phys. Chem. C, 112 (2008) 11408-11420.

[32] L. Lee, F. Zaera, J. Phys. Chem. B, 109 (2005) 2745-2753.

[33] A. McCue, A. Guerrero-Ruiz, C. Ramirez-Barria, I. Rodríguez-Ramos, J. A. Anderson, J. Catal. 355 (2017) 40-52.

[34] B. Bachiller-Baeza, A. Iglesias-Juez, E. Castillejos-López, A. Guerrero-Ruiz, M. Di Michiel, M. Fernández-García, I. Rodríguez-Ramos, ACS Catal. 5 (2015) 5235–5241.

[35] D. Albani, M. Shahrokhi, Z. Chen, S. Mitchell, R. Hauert, N. López, J. Pérez-Ramírez, Nat. Commun. 9 (2018) 2364.

[36] G. Kresse, J. Phys. Rev. B 54 (1996) 11169.

[37] P. E. Blochl, Phys. Rev. B 50 (1994) 17953.

[38] J. P. Perdew, K. Burke, M. Ernzerhof, Phys. Rev. Lett. 78 (1997) 1396.

[39] G. Henkelman, B. P. Uberuaga, H. Jónsson, J. Chem. Phys. 113 (2000) 9901−9904.

[40] Y. Liu, A. J. McCue, J. Feng, S. Guan, D. Li, J. A. Anderson, J. Catal. 364 (2018) 204–215.

[41] B.N. Bobylev, M.I. Farberov, D.I. Epshtein, G.M. Bogdanov, Pet. Chem. USSR, 14 (1974) 174-180.

[42] B. S. Akpa, C. D. Agostino, L. F. Gladden, K. Hindle, H. Manyar, J. McGregor, R. Li, M. Neurock, N. Sinha, E.H. Stitt, D. Weber, J. A. Zeitler, D. W. Rooney, J. Catal. 289 (2012) 30-41.

[43] F. Huang, Y. Deng, Y. Chen, X. Cai, M. Peng, Z. Jia, P. Ren, D. Xiao, X. Wen, N. Wang, H. Liu, D. Ma, J. Am. Chem. Soc. 140 (2018) 13142−13146.

[44] Q. Feng, S. Zhao, Y. Wang, J. Dong, W. Chen, D. He, D. Wang, J. Yang, Y. Zhu, H. Zhu, L. Gu, Z. Li, Y. Liu, R. Yu, J. Li, Y. Li, J. Am. Chem. Soc. 139 (2017) 7294-7301.

[45] M. Jørgensen, H. Grönbeck, J. Am. Chem. Soc. 141 (2019) 8541−8549.